12-1-2016

TLR8 Couples SOCS-1 and Restrains TLR7-Mediated Antiviral Immunity, Exacerbating West Nile Virus Infection in Mice

Amber M. Paul
University of Southern Mississippi

Dhiraj Acharya
University of Southern Mississippi

Linda Le
University of Southern Mississippi

Penghua Wang
Yale University School of Medicine

Dobrivoje S. Stokic
Methodist Rehabilitation Center

See next page for additional authors

HHS Public Access

Author manuscript

J Immunol. Author manuscript; available in PMC 2017 December 01.

Published in final edited form as:

J Immunol. 2016 December 1; 197(11): 4425–4435. doi:10.4049/jimmunol.1600902.

TLR8 couples SOCS-1 and restrains TLR7-mediated antiviral immunity exacerbating West Nile virus infection in mice

Amber M. Paul[1], **Dhiraj Acharya**[1], **Linda Le**[1], **Penghua Wang**[2,3], **Dobrivoje S. Stokic**[4], **A. Arturo Leis**[4], **Lena Alexopoulou**[5], **Terrence Town**[6], **Richard A. Flavell**[7,8], **Erol Fikrig**[2,8], and **Fengwei Bai**[1,*]

[1]Department of Biological Sciences, The University of Southern Mississippi, Hattiesburg, MS 39406, USA

[2]Section of Infectious Diseases, Department of Internal Medicine, Yale University School of Medicine, New Haven, CT 06520, USA

[3]Department of Microbiology & Immunology, School of Medicine, New York Medical College, Valhalla, NY, USA

[4]Center for Neuroscience and Neurological Recovery, Methodist Rehabilitation Center, Jackson, MS 39216, USA

[5]Centre d'Immunologie de Marseille-Luminy, Aix Marseille Université UM2, Inserm, U1104, CNRS UMR7280, 13288 Marseille, France

[6]Zilkha Neurogenetic Institute, Keck School of Medicine of the University of Southern California, Los Angeles, CA, USA

[7]Department of Immunobiology, Yale University School of Medicine, New Haven, CT 06520 USA

[8]Howard Hughes Medical Institute, New Haven, CT 06520, USA

Abstract

West Nile virus (WNV) is a neurotropic, single-stranded RNA (ssRNA) flavivirus that can cause encephalitis, meningitis, and death in humans and mice. Human Toll-like receptor (TLR) 7, 8, and mouse TLR7 recognize viral ssRNA motifs and induce antiviral immunity. However, the role of mouse TLR8 in antiviral immunity is poorly understood. Here, we report that TLR8 deficient (*Tlr8*$^{-/-}$) mice were resistant to WNV infection compared to wild-type (WT) controls. Efficient WNV clearance and moderate susceptibility to WNV-mediated neuronal death in *Tlr8*$^{-/-}$ mice was attributed to overexpression of *Tlr7* and an interferon-stimulated gene *Isg-56* expression, while reduced expression of the pro-apoptotic gene coding Bcl2-associated X protein (*Bax*) was observed. Interestingly, suppressor of cytokine signaling -1 (SOCS-1) directly associated with TLR8, but not with TLR7, indicating a novel role for TLR8 regulation of SOCS-1 function, while selective siRNA knockdown of *Socs-1* resulted in induced *Isg-56* and *Tlr7* expression following

[*]**Corresponding Author:** Fengwei Bai, Ph.D., Department of Biological Sciences, The University of Southern Mississippi, 118 College Drive # 5018, Hattiesburg, MS 39406, USA. fengwei.bai@usm.edu; Telephone 601-266-4748; Fax: 601-266-5797 .

Conflict of Interest. The authors declare no competing or conflicting interests.

WNV infection. Collectively, we report that TLR8 coupling with SOCS-1 inhibits TLR7-mediated antiviral immunity during WNV infection in mice.

Introduction

West Nile virus (WNV) is a mosquito-borne, single-stranded (ss) RNA flavivirus that has caused significant morbidity and mortality in North America (1). In humans, WNV can cause a wide range of debilitating illnesses, from febrile-like illness to viral encephalitis, paralysis, and even death (2). However, the pathogenesis of WNV is still not clearly defined, and there is no approved WNV vaccine or specific antiviral therapeutic available for human use.

After mosquito inoculation, WNV initially infects skin Langerhans cells and macrophages, and then further replicates in draining lymph nodes, spleen, and other peripheral organs generating transient viremia. Prior to the development of specific humoral or T cell-mediated immune responses, WNV may enter into the spinal cord and brain, leading to symptomatic neuronal dysfunction. Therefore, early control of WNV infection of neurons heavily relies on innate immunity. Toll-like receptors (TLRs) are a family of innate pattern recognition receptors (PRRs) that are located on either plasma-, or within endosomal-membranes of host cells. WNV has been reported to be recognized by TLR3 (3) and TLR7 (4), which play important roles during antiviral immunity by initiating a variety of cellular signal transduction cascades, including the Myd88 dependent and independent cascades to control infection (3-8), and initiates the expression of interferon stimulated genes (*Isg*), which can inhibit viral replication and transcription/translation of viral proteins through various antiviral mechanisms (9, 10). On the other hand, TLR signaling can be compromised when single nucleotide polymorphisms (SNPs) are present in *Tlr2, Tlr3, Tlr4, Tlr7, Tlr8, and Tlr9* genes that have been associated with defective antiviral immunity in human immunodeficiency virus (11, 12), herpes simplex virus type 2 (13), and Rift Valley fever virus (14) infections.

Human TLR8 can recognize viral ssRNA, but mouse TLR8 has been described as non-functional (15-17) and its natural ligand remains unknown. This may be due to a deletion of five amino acids in the leucine-rich repeat ectodomain of TLR8 in mice, which is a region critical for recognition of viral ssRNA (18, 19). Although somewhat controversial (20), one study has suggested that mouse TLR8 could recognize specific DNA motifs in vaccinia virus (21), while another report has suggested that TLR8 recognizes a combination of imidazoquinoline and poly-T oligodeoxynucleotides (22), however the natural ligand of mTLR8 still remains elusive. Interestingly, overexpression of murine TLR8 neither activates interferon regulatory factor 3 (IRF-3) nor interferon-α in HEK293T cells, suggesting TLR8 may inhibit the type I interferon pathway (23). In addition, TLR8 knockout (*Tlr8*$^{-/-}$) mice develop lupus-like autoimmunity due to increased TLR7 function (24-26). Therefore, the function of TLR8 in mice is complicated and its role during antiviral immunity needs to be further investigated.

Signal transduction pathways that are triggered following cytokine and PRR engagement must be tightly regulated to prevent aberrant immune responses. Regulation is maintained

through protein tyrosine phosphatases, protein inhibitors of activated STATs (PIAS), and suppressors of cytokine signaling (SOCS) proteins (27, 28). *Socs* genes are expressed at a relatively low levels in an inactivated state, but are rapidly transcribed following TLR or cytokine engagement (28). For instance, *Socs-1* and *Socs-3* are induced following WNV infection, possibly acting as neuroprotective responses within the brain to regulate aberrant inflammation (29). SOCS-1 has been shown to inhibit STAT-1 signaling of IFNα (30), suggesting SOCS-1 regulates type I IFNs. Antiviral immunity involves the secretion of type I IFNs, such as IFNα and IFNβ, from viral-infected cells and act through a paracrine or autocrine mechanism, which engages the JAK/STAT signal transduction pathway to induces a multitude of antiviral molecules that directly or indirectly inhibit viral infection (31). Interferon stimulated gene-56 (*Isg-56,* ISG-56/IFIT-1) has been shown to be induced by active STAT-1/2 and IRF-3/5/7/9 molecules following type I IFN signaling transduction (32) and protects neurons from WNV infection (33, 34).

Herein, we report that TLR8 partners with SOCS-1 to control TLR7-mediated antiviral immunity in the central nervous system (CNS) of mice during WNV infection.

Materials and Methods

Ethics statement and biosafety

All animal experimental procedures were reviewed and approved by the Institutional Animal Care and Use Committees at The University of Southern Mississippi (USM) and Yale University. All the *in vitro* experiments and animal studies involving live WNV were performed by certified personnel in biosafety level 3 (BSL3) laboratories following standard biosafety protocols approved by USM and Yale University Institutional Biosafety Committees.

Viruses, animals, cells, and chemicals

WNV isolate (CT2741) was kindly provided by Dr. John F. Anderson at the Connecticut Agricultural Experiment Station. To prepare virus stocks, WNV was propagated and titered in Vero cells (ATCC CCL-81) by a plaque assay, as previously described (35). *Tlr8*$^{-/-}$ mouse breeding pairs were provided by Dr. Richard A. Flavell and wild-type (WT, C57BL/6J) control mice were purchased from the Jackson Laboratories (Bar Harbor, ME). Seven week-old WT and *Tlr8*$^{-/-}$ mice were inoculated intraperitonealy with 2000 plaque forming units (PFUs) of WNV in 1% gelatin for survival analysis and tissue collection, according to previous publications (36-38).

BMDCs were isolated from WT or *Tlr8*$^{-/-}$ mice (3 to 6 month old) and cultured as previously described (39). Briefly, mouse bone marrow cells were collected from femurs and grown in DMEM supplemented with 10% FBS, 2% plasmacytoma cell medium containing GM-CSF (J588L), 1% Pen/Strep, 1% L-glu and 50 μM of β-mercaptoethanol until maturation (11 days). Mature BMDCs were either infected with WNV or stimulated with the TLR7 ligands CL264 (Invitrogen) or Loxoribine (Invitrogen).

Murine primary mixed neuronal cultures were isolated from WT and *Tlr8*$^{-/-}$ mice (6 to 12 month old), as previously described with some modifications (40). Briefly, whole brains

were isolated in ice-cold HEPES-buffered saline (HBS), minced and triturated in Papain (2 mg/ml) in HBS and incubated for 15 minutes at 37°C. Following incubation, cells were plated on poly-ornithine pre-treated plates for 20 minutes at 37°C, followed by a gentle wash with HBS to remove cellular debris. Cells were cultured in DMEM:F12 (1:1) medium (Thermo Scientific) supplemented with 1% Pen/Strep, 10% FBS, 1% L-glu, and glucose (4.5g/l). On day 11, supernatant was removed and replaced with Neurobasal®-A media (Life Technologies) supplemented with 2% B-27 (Life Technologies), 10% FBS, 1% L-glu and 1% Pen/Strep. The mature neurons were infected with WNV (MOI = 1) for 24 or 48 hr.

Murine Neuro-2a cell line (CCL-131) and the murine macrophage cell line, RAW 264.7 cells (TIB-71) were purchased from ATCC and were maintained in DMEM containing 10% FBS and 1% Pen/Strep at 37°C with 5% CO_2.

TLR7 and TLR8 ligands CL264, CL075, loxibrine and PolydT were all purchased from Invivogen and used at indicated concentrations and time points.

Interferon bioassay

Bioactive type I IFN in culture supernatant was analyzed by a previously described method (41) that measured IFN pre-treated protection against encephalomyocarditis virus (EMCV) in a susceptible cell line (L929, ATCC). Briefly, culture supernatant collected from WT and *Tlr8*$^{-/-}$ mice BMDCs that were infected *in vitro* with WNV for 24 hr (MOI = 5) were UV-inactivated (10 minutes at 120 mJ/s). The crude, UV inactivated supernatant was added to monolayers of L929 cells (cultured in DMEM supplemented with 10% FBS and 1% Pen/Strep) in 96-well flat bottom plates. Following incubation for 14 h at 37°C, medium was removed and cells were infected with EMCV (MOI = 10) for 7 hr. ECMV-mediated cell death was measured using a CellTiter 96 aqueous cell proliferation assay kit (Promega) and an ELx808 ultra microplate reader (BIO-TEK Instruments, Inc.). The percentage (%) of protected cells was calculated as described (41), according to the following formula: (optical density at 492 nm [OD_{492}] of supernatant-treated EMCV-infected cells / OD_{492} of non-EMCV-infected cells × OD_{492} of EMCV-infected cells) / (OD_{492} of non-EMCV-infected cells) × 100%).

Quantitative PCR (qPCR)

Mouse tissues, blood, or cultured cells were collected for total RNA extraction with TRIreagent (Molecular Research Center, Inc.) and converted into first strand cDNA using the iSCRIPT™ cDNA synthesis kit (Bio-Rad). qPCR assays were performed using iTAQ™ polymerase supermix for probe-based assays (Bio-Rad) or iQ™ SYBR® Green Supermix polymerase (Bio-Rad). WNV-envelope (*WNV-E*) gene and mouse gene primers and probes sequences were adapted according to previous publications: *WNV-E* (4), *β-Actin* (42), *Tlr7* (24), *Irf-7* (43), *Ifn-α* (43), *Isg-56* (43), *Isg-54* (44), *Isg-49* (44), *Ifn-β* (43), and *Socs-1* (45). Primers were designed for murine *Bax*, forward 5'-TGCTAGCAAACTGGTGCTCA-3' and reverse 5'-TAGGAGAGGAGGCCTTCCCAG-3'. Data were presented either as relative fold change (RFC) by the $2^{-\Delta\Delta CT}$ method, using *β-actin* as a housekeeping gene, or was expressed as a ratio of target gene to *β-actin* copy numbers. All the primers and probes were synthesized either by Integrated DNA Technologies or Applied Biosystems.

RNA interference

siRNAs were designed using the Thermo Scientific siRNA designing tool (siDESIGN Center) targeting murine *Isg-56* (10nM, 5'-GUAAGUAGCCAGAGGAAGGUGAUGCUU-3') or a scrambled sequence (5'-ACUACUUCAGGUGUGAGCUAAUAUACC-3') and were transfected with RNAiMAX Lipofectamine reagent (Life Technologies) into Neuro-2a cells in OPTI-MEM medium (Life Technologies) for 20 minutes. DMEM containing 2% FBS was then added and cell were cultured for 24 hr. Following incubation, media was removed and cells were infected with WNV (MOI = 5) for 48 hr. Cells were then collected for qPCR and flow cytometric analyses.

Murine siRNAs targeting murine *Socs-1* (Santa Cruz Biotechnologies) were transfected into RAW 264.7 cells (6×10^5 cells/ml) following manufactures recommendation, with some minor changes. Briefly, lipoplexes were prepared in OPTI-MEM media (Life Technologies) by mixing siRNA (25 nM) and transfection reagent (Santa Cruz Biotechnology) for 30 minutes. Cells and lipoplexes were mixed in 12-well plates and incubated in OPTI-MEM for 24 hr. DMEM containing 2% FBS was added to the cells followed by infection with WNV (MOI = 0.1) and cells were cultured for and additional 24 hr. Following infection, cells were collected and prepared for qPCR analysis.

Immunocytochemistry and immunofluorescence assays

Murine BMDCs were isolated, and plated at 3×10^5 cells / well and infected with WNV at day 11. Infected cells were then fixed with 4% paraformaldehyde (PFA) in PBS for 15 minutes at room temperature (RT). The cells were washed with PBS, blocked with 2% normal goat serum (Life Technologies) containing 0.4% Triton-X for 1 hr at room temperature (RT), and probed with monoclonal mouse-anti-flavivirus glycoprotein E IgG antibody (4G2, ATCC D1-4G2-4-15 HB-112) overnight at 4°C. The cells were then washed with PBS and probed with goat polyclonal anti-mouse-HRP IgG (KPL) for 2 hr at RT. Immuno-positive cells were developed with TrueBlue peroxidase substrate (KPL). Images were taken using an Axiostar Plus light microscope (Zeiss) and mean pixel intensity was quantified using ImageJ (version 1.48), as previously described (46).

Similarly, primary neurons were isolated from mice, infected with WNV, and fixed as described above. After a 1 hr blocking step at RT with 2% normal goat serum containing 0.4% Triton-X, neurons were probed with mouse monoclonal-anti-WNV-E (1:50, Abcam) and rabbit polyclonal anti-ISG-56 antibodies (1:100) overnight at 4°C. The cells were then washed with PBS and probed with polyclonal goat-anti-mouse-FITC IgG (eBioscience) and polyclonal goat-anti-rabbit-DyLight594 IgG (Thermo Scientific) for 2 hr at RT. The cells were then washed with PBS, mounted using Vectashield® mounting medium containing DAPI, and imaged as above.

For brain immunohistochemistry, WNV infected WT and *Tlr8*$^{-/-}$ mice were euthanized (day 6 p.i) and perfused with ice-cold PBS. Half brain was fixed overnight in 4% PFA, followed by frozen tissue cyroprotection with daily changes in 10%, 20%, and 30% sucrose in PBS. Brain tissues were frozen in Tissue-Plus™ O.C.T. buffer (Fisher Healthcare) and midsagittal

sections (10 μm) were cut using a Tissue-Tek®Cryo3® microtome/cryostat (Sakura) and mounted on pre-cleaned Superfrost® Plus microscope slides (Fisher Scientific). Apoptotic measurement of brain tissue was detected by TACS® 2 TdT-Fluor *in situ* apoptosis detection kit (Trevigen) following manufacturer's recommendations and images were acquired using a confocal LSM 510 microscope (Zeiss).

Immunoblotting and immuoprecipitation

Mouse whole brains were prepared with lysis buffer containing 50 mM Tris-HCl, 150 mM NaCl, and 0.25% sodium dodecyl sulfate (SDS), 0.25% Sodium Deoxycholate, 1 mM EDTA and 1% Proteinase inhibitor cocktail (Sigma P8340). Protein concentration in lysates was quantified by a Bradford Assay (Bio-Rad) and cell lysates were mixed with 2× Laemmli buffer (Bio-Rad) containing 0.1% β-mercaptoethanol (Sigma), boiled at 95°C for 5 minutes, and rapidly spun down. Whole-cell protein lysates (5-10 μg/well) were separated by polyacrylamide gel electrophoresis and were transferred to a nitrocellulose membrane (Bio-Rad). The membrane was blocked with 5% bovine serum albumin (BSA) for 1 hr and probed with rabbit polyclonal anti-TLR7 (Cell Signaling Technology), rabbit polyclonal anti-ISG-56 (Pierce Antibodies), rabbit monoclonal anti-STAT-1 (Cell Signaling Technology), rabbit monoclonal anti-IRF-7 (Abcam) antibodies in 5% BSA overnight at 4°C. The immunolabeled membrane was then probed with secondary HRP-conjugated goat anti-rabbit IgG (Jackson ImmunoResearch Laboratories, Inc.) for 2 hr. *β*-Tubulin-HRP (Cell Signaling Technology) was used as a loading control. Membranes were developed with SuperSignal West Pico Chemiluminescence Substrate (Thermo Scientific) and images were acquired using a ChemiDoc™ XRS+ System (Bio-Rad).

For immunoprecipitation, Neuro-2a cell lysates were prepared as mentioned above, and were mixed with rabbit polyclonal anti-TLR7 (1:50, Cell Signaling Technology) or rabbit polyclonal anti-TLR8 (1:50, Sigma) antibodies for 2 hr at RT, washed in 1× TBS containing 0.05% Tween 20, and 0.5 M NaCl, and were mixed with Dynabeads Protein G (Life Technologies) for an additional 1 hr. Samples were then washed and resuspended in 2× Laemmli buffer containing 0.1% β-mercaptoethanol, boiled at 95°C for 5 minutes, and rapidly spun down. Proteins from whole-cell lysates were separated by polyacrylamide gel electrophoresis and transferred to a nitrocellulose membrane. Membranes were then probed with a rabbit polyclonal anti-SOCS-1 antibody (1:1000, Sigma) in 5% BSA overnight at 4°C, followed by probing with a secondary peroxidase-conjugated goat anti-rabbit IgG (Jackson ImmunoResearch Laboratories, Inc.) for 2 hr, and developed as above. Loading control input bands were detected following back incubation with the rabbit polyclonal anti-TLR8 antibody (Sigma).

Flow cytometry

TLR7 expression in blood cells—Blood samples were collected in EDTA-coated tubes from WNV infected WT and *Tlr8*$^{-/-}$ mice by retro-orbital bleeding and red blood cells (RBC) were lysed by adding RBC lysis buffer (Sigma). Blood cells were washed two times to remove lysed RBCs and resuspended in flow cytometry buffer (PBS +2% FBS) at 5 × 10^5 cells/ ml. Cells were probed overnight at 4°C with rabbit polyclonal anti-TLR7 antibody (Cell Signaling Technology), washed two times with flow buffer, and probed with secondary

goat-anti-rabbit-DyLight594 IgG (Thermo Scientific) for 2 hr at RT. Cells were then washed two times and analyzed in a BD LSRFortessa flow cytometer (BD Biosciences) and data were acquired using BD FACSDIVA™ version 7.0 (BD Biosciences). Cells probed only with secondary antibody were used as controls for fluorescence gating.

TLR7, WNV antigen and IFNα in BMDCs—WT and *Tlr8*$^{-/-}$ BMDCs were infected with WNV (MOI = 5) for 24 hr, as described above. The cells were fixed with 2% PFA and permeabilized with PBS +0.05% Tween-20 (permeabilization buffer). The cells were incubated overnight with mouse monoclonal anti-WNV-Envelope IgG2b (1:100, Abcam) antibody, rat monoclonal anti-IFNα IgG1 (1:100, Abcam), or rabbit polyclonal anti-TLR7 (1:100, Cell Signaling Technology) followed by two washes with permeabilization buffer, and probed with a secondary goat-anti-mouse-IgG antibody conjugated to FITC (Santa Cruz Biotechnology), goat-anti-rat-IgG antibody conjugated to Alexa Fluor® 555 (Molecular Probes), or goat-anti-rabbit-IgG antibody conjugated to DyLight594 (Thermo Scientific), respectively, for 2 hr at RT in dark. For WNV antigen detection, cells were washed two times with permeabilization buffer, and resuspended in DAPI (100 μM) for 10 minutes, then analyzed FITC mean fluorescent expression (MFI) with a flow cytometer (BD LSRFortessa). DAPI expression was analyzed with a microplate reader (BioTek® SynergyHI) using Gen5 (version 2.07) software to determine the ratio of FITC^{+} MFI normalized to DAPI^{+} cells.

Secreted IFNα in cell medium—UV inactivated supernatant collected from WT and *Tlr8*$^{-/-}$ BMDCs were incubated with rat monoclonal anti-IFNα antibody (1:50) over night at 4°C, on a rocker to create immune complex formation. In a separate tube, Dynabeads Protein G (Life Technologies) were washed in buffer (TBS + 0.05% Tween-20, 0.5M NaCl) and added to the supernatant containing IFNα antibodies for 1 hr at RT. The beads were then magnetically separated from the remaining supernatant, washed, and secondary anti-rat-antibody conjugated to AlexaFluor® 555 (1:1000) was added. After incubation for 2 hr at RT, the beads were detached from the immune complexes with an elution buffer (0.1M glycine, pH 2.0) and neutralized in Tris-HCL (pH 9.0) buffer. The MFI of the beads was analyzed by flow cytometry, as above.

Apoptosis Assay—Apoptosis was measured using a modified annexin V and propidium iodide (PI) apoptosis assay (47). Briefly, Neuro-2a cells were collected and resuspended in annexin V binding buffer followed by staining with annexin V conjugated to Alexa Fluor® 488 (Molecular Probes) and PI (Sigma). Cells were then washed with annexin V binding buffer and fixed in a 1% PFA for 10 minutes on ice and then were incubated in RNase A (50 μg/ml, Sigma) for 15 minutes at 37°C, washed twice in PBS, and analyzed by flow cytometry.

Statistical analyses

Data were compared with either a Student's *t*-test or two-way analysis of variance with Bonferroni post-hoc analysis. Survival curves were analyzed using a Kaplan-Meier analysis. All statistical analyses were performed by using GraphPad Prism software (version 6.0).

Results

TLR8 signaling in mice facilitates WNV infection

Our previous report demonstrated that TLR7 signaling protects mice from lethal WNV infection (4) and *Tlr7* expression is up-regulated in TLR8 deficient (*Tlr8*$^{-/-}$) mice (24). To investigate the potential role of TLR8 during WNV infection in mice, we challenged *Tlr8*$^{-/-}$ and WT mice intraperitoneally (i.p.) with 2000 plaque forming units (PFU) of WNV and monitored mice twice daily for morbidity and mortality for up to 21 days. The Kaplan-Meier survival analysis shows that 52% of *Tlr8*$^{-/-}$ and 26% of WT mice survived of lethal WNV infection (Fig. 1A), indicating that TLR8 signaling facilities WNV infection in mice. To further confirm this observation, we measured viral burden in the blood and brains of WNV-infected mice by quantitative polymerase chain reaction (qPCR). Consistent with the survival data, the qPCR results show the lower expression of *WNV-E* transcripts in blood of *Tlr8*$^{-/-}$ mice compared to WT controls at day 4 and the brain at days 4 and 6 post-infection (p.i.) (Fig. 1B-D). These results indicate that TLR8 signaling in mice plays a negative role in WNV immunity by facilitating WNV replication. Type I interferons (IFN) play essential roles in viral clearance and control of WNV burden in mice (48, 49). Therefore we assessed the expression of type I IFNs in blood samples collected from WNV-infected *Tlr8*$^{-/-}$ and WT mice at day 1 to day 4 p.i. by qPCR. The results showed that *Tlr8*$^{-/-}$ mice have increased expression of *Ifn-α* at days 1 to 4, and *Ifn-β* at days 1 and 2, compared to WT controls following WNV infection (Fig. 1E and F). In addition, IFN regulatory factor-7 (*Irf-7)* and IFN stimulated gene-56 (*Isg-56*) measured in blood of WNV-infected *Tlr8*$^{-/-}$ mice showed an increasing trend in gene expression (Fig. 1G and H). In summary, these results indicate that TLR8 facilitates WNV infection in mice possibly due to the down-regulation of type I IFN-dependent antiviral response.

TLR8 in mice negatively regulate TLR7-mediated WNV immunity

Since naïve *Tlr8*$^{-/-}$ mice express higher levels of *Tlr7* (24), we measured the expression of TLR7 in blood leukocytes collected from WNV-infected WT and *Tlr8*$^{-/-}$ mice by flow cytometry at day 1 post-WNV infection. The results indicate an increased expression of TLR7 in leukocytes of WNV-infected *Tlr8*$^{-/-}$ mice compared to WT controls (Fig. 2A). To further investigate the potential role of TLR8 in regulating the expression of *Tlr7* during WNV infection, we infected bone marrow derived dendritic cells (BMDCs) from *Tlr8*$^{-/-}$ and WT mice with WNV (multiplicity of infection, MOI = 5) *in vitro* and measured the expression of *Tlr7* by qPCR. In line with the *in vivo* results, the qPCR results showed a higher basal expression level of *Tlr7* in BMDCs from *Tlr8*$^{-/-}$ mice compared to WT controls, which was further amplified following WNV infection, indicating overexpressed *Tlr7* in the absence of TLR8 (Fig. 2B). Consistent with this, we also confirmed TLR7 expression on BMDCs from *Tlr8*$^{-/-}$ mice was further increased following WNV infection at the protein level by flow cytometry (supplemental (s)Fig. 1A). To assess the antiviral function of *Tlr7* overexpression, we stimulated BMDCs from *Tlr8*$^{-/-}$ and WT mice with the TLR7-specific ligand CL264 (5 μg/ml) and measured the expression of type I IFN by qPCR. We found higher levels of *Ifn-α* (Fig. 2C) and *Ifn-β* (sFig. 1B) expression in BMDCs generated from *Tlr8*$^{-/-}$ mice compared to WT controls at multiple time points, suggesting that overexpression of TLR7 in *Tlr8*$^{-/-}$ mice may induce stronger antiviral immunity. To

confirm this, we infected BMDCs from *Tlr8*$^{-/-}$ and WT mice with WNV (MOI = 5) or an alphavirus, chikungunya virus (CHIKV, MOI = 5), and assessed the transcript levels of *Ifn-α* and *Ifn-β* at 24 hr post-infection (p.i.) by qPCR. The results show higher expression of *Ifn-α* (Fig. 2D) and *Ifn-β* (sFig. 1C) in BMDCs generated from *Tlr8*$^{-/-}$ mice than WT controls in response to both type of infections, WNV or CHIKV, suggesting a response not only specific to WNV. In addition, intracellular and secreted IFN-α was also shown to be increased in *Tlr8*$^{-/-}$ BMDCs as compared to WT controls following WNV infection in a flow cytomertic assay (Fig. 2E and F). Moreover, we measured gene expression of signaling proteins involved in the type I IFN response, and found that WNV infection significantly induced the expression of both *Irf-7* and *Isg-56* in *Tlr8*$^{-/-}$ BMDCs compared to WT controls at 24 hr p.i. with WNV (Fig. 2G and 2H). To further confirm higher expression of type I IFN in the absence of TLR8, we measured bioactive type I IFN in cell culture supernatant of WNV-infected *Tlr8*$^{-/-}$ and WT BMDCs, as previously described (41). The IFN bioassay further confirmed that BMDCs generated from *Tlr8*$^{-/-}$ mice produced more IFN than those from WT controls during WNV infection (Fig. 2I). Since BMDCs generated from *Tlr8*$^{-/-}$ mice have increased antiviral immunity, we expected these cells to be more efficient in controlling WNV infection. Indeed, we found that BMDCs from *Tlr8*$^{-/-}$ mice are more resistant to WNV infection *in vitro* compared to those from WT mice, as measured by reduced WNV antigen expression (Fig. 2 J and K, and sFig. 1D and E). In summary, these results show that TLR8 signaling in mice down-regulates the expression of *Tlr7*, which results in reduced antiviral immune response against WNV infection.

TLR8 negatively regulates antiviral immunity within the murine central nervous system (CNS)

WNV can cause severe CNS infection and can lead to injury and death of neurons in both mice and humans. Since we observed reduced viral burden in the brains of WNV-infected *Tlr8*$^{-/-}$ mice and increased expression of *Tlr7* and other antiviral genes in *Tlr8*$^{-/-}$ BMDCs infected *in vitro* with WNV, we asked whether TLR8 also regulates antiviral immunity in the brains of WNV-infected mice. On day 4 post-WNV infection (2000 PFU/mouse, i.p.), *Tlr8*$^{-/-}$ and WT mice were euthanized, perfused with ice-cold PBS, and whole brains were collected for qPCR and western blotting analyses of TLR7 and other antiviral molecules. Consistent with the results from BMDC, uninfected *Tlr8*$^{-/-}$ mice exhibited increased basal expression of *Tlr7* in brains compared to WT controls, which was further increased following WNV infection (Fig. 3A). These results suggest that increased *Tlr7* expression in brains of *Tlr8*$^{-/-}$ mice may result in better capability to recognize and respond to neuroinvasive WNV. To further test this, we measured the expression of *Irf-7, Ifn-α* and *Ifn-β* in brain tissues collected from WNV-infected *Tlr8*$^{-/-}$ and WT mice by qPCR, and the results indicated slightly higher expression of *Irf-7* (Fig. 3B) and a trend for increased expression of *Ifn-α* (Fig. 3C), while the expression of *Ifn-β* remained unaltered (data not shown). Since type I IFNs were not robustly increased in the brains of *Tlr8*$^{-/-}$ mice, but viral burden was significantly reduced (Fig. 1C and D), we sought to examine if *Tlr8*$^{-/-}$ mice overexpress other antiviral genes. To test this, we examined the expression of *Isg-56, Isg-54*, and *Isg-49.* Interestingly, the expression of *Isg-56* was increased (Fig. 3D) in *Tlr8*$^{-/-}$ mice brains following WNV infection was enhanced, while the expression of *Isg-54* and *Isg-49* were not significantly altered (data not shown). In addition, we also confirmed higher

expression TLR7, ISG-56, IRF-7 and STAT-1 in brain lysates of WNV-infected *Tlr8*$^{-/-}$ mice at protein levels by an immunoblotting assay (Fig. 3E). Together, these results confirm that *Tlr8*$^{-/-}$ mice express higher level of TLR7 in brain tissue, which may lead to strong antiviral responses via increased expression of ISG-56, IRF-7 and STAT-1.

We next analyzed the expression of *Tlr7* and antiviral genes in primary mixed neuronal cultures isolated from WNV infected (MOI = 1, 24 hr) WT and *Tlr8*$^{-/-}$ mice whole brain homogenates *in vitro*. The qPCR analysis indicate that *Tlr7*, *Irf-7*, and *Ifn-α* were all increased following WNV infection in *Tlr8*$^{-/-}$ neurons compared to WT controls (Fig. 3F-H), suggesting that the TLR7-mediated IFN signaling pathway may increase neuronal resistance against WNV infection in *Tlr8*$^{-/-}$ mice. We further assessed if the expression of IFN-stimulated genes were also altered in WNV-infected *Tlr8*$^{-/-}$ neurons by qPCR. Consistent with *in vivo* brain tissue results (Fig. 3D), we found increased expression of *Isg-56* (Fig. 3I), along with increased *Isg-54* and *Isg-49* in the *Tlr8*$^{-/-}$ neurons infected *in vitro* with WNV compared to WT controls (data not shown). In line with increased antiviral immunity, immunofluorescence microscopy show reduced WNV antigen and increased ISG-56 expression in WNV-infected *Tlr8*$^{-/-}$ neurons compared to WT controls (Fig. 3J and K). In summary, these results indicate that TLR8 inhibits antiviral immunity against WNV infection leading to enhance viral replication within the CNS.

TLR8 expression results in increased WNV-induced apoptosis that is CNS region-specific

One of the major cell death pathways that occur in WNV neuroinvasive disease is apoptosis, in particular via the induction of the apoptotic mediated gene, Bcl-2 associated X protein (*Bax*) (50, 51). To examine the degree of WNV-mediated cellular apoptosis in *Tlr8*$^{-/-}$ and WT brain tissue, whole brains were isolated at day 6 p.i. and were analyzed by a TUNEL assay. The TUNEL assay showed that *Tlr8*$^{-/-}$ mice had significantly reduced cell death of WNV-permissive Purkinje neurons of the cerebellum (52-57) compared to WT controls (Fig. 4A), with no observable differences in any other regions of the brain. Interestingly, we found that the gene expression of *Bax* (Fig. 4B), along with antiviral genes *Isg-56* and suppressor of cytokine signaling (*Socs-1)* were significantly altered only in the spinal cords and cerebellar regions of *Tlr8*$^{-/-}$ mice at day 4 p.i. (data not shown), suggesting that antiviral immunity confined viral-induced apoptosis within these regions of the brain. In line with this, previous reports have suggested that the expression (56) and neuroprotective role of ISG-56 does indeed localize to these specific region of CNS (34). WT and *Tlr8*$^{-/-}$ neurons infected with WNV (MOI = 1) for 24 hr *in vitro* were also analyzed for *Bax* expression by qPCR, indicating reduced neuronal Bax-dependent apoptosis occurs in *Tlr8*$^{-/-}$ mice following WNV infection (Fig. 4C). These results indicate that TLR8 signaling counteracts antiviral immunity, possibly by down-regulation of *Isg-56* expression, favoring WNV-induced neuronal death.

Since higher expression of ISG-56 in brains of *Tlr8*$^{-/-}$ mice following WNV infection is associated with the reduced *Bax* expression, we tested if the *Bax*-mediated apoptosis is dependent on *Isg-56* expression. For this, we used siRNAs to knockdown *Isg-56* in mouse Neuro-2a cells, and assessed *Bax* expression and apoptosis following WNV infection *in vitro*. *Isg-56*-specific siRNAs were transfected into Neuro-2a cells for 24 hr and the cells

were further infected with WNV (MOI = 5) for an additional 48 hr. The efficiency of siRNAs to knockdown *Isg-56* expression was confirmed by qPCR in WNV-infected Neuro-2a cells (Fig. 4D). Interestingly, knockdown of *Isg-56* leads to increased replication of WNV (Fig. 4E) and the expression of *Bax* (Fig. 4F), suggesting that WNV replication may be inhibited by ISG-56 expression. To test if apoptosis is the direct consequence of increased *Bax* expression in siRNA-*Isg-56*-transfected Neuro-2a cells, we stained WNV-infected Neuro-2a cells with annexin-V and measured apoptosis by flow cytometry. The results confirmed that knocking down *Isg-56* expression increased apoptosis of WNV-infected Neuro-2a cells (Fig. 4G and H). Collectively, these data indicate that ISG-56 is an essential antiviral molecule that controls WNV-induced neuronal apoptosis.

TLR8 regulates SOCS-1 signaling, which controls *Isg-56* and *Tlr7* expression

Socs-1 has been shown to be induced by WNV (29) and its expression inhibits antiviral responses, such as type I IFNs (58). We found that the expression of *Socs-1* was significantly reduced in brain tissue and neurons in *Tlr8*$^{-/-}$ mice following WNV infection (Fig. 5A and B), suggesting that TLR8 regulates *Socs-1* expression during WNV infection. To test if TLR8 directly regulates SOCS-1 function, we performed an immunoprecipitation (IP) assay in Neuro-2a cells in the presence of various TLR7, and suspected mouse TLR8 ligands (22). Interestingly, we found that SOCS-1 co-precipitates with TLR8, but not TLR7 (Fig. 5C), even in the presence of TLR7 and TLR8 ligation. These results suggest that TLR8 may directly control SOCS-1 function within neurons in mice. To test if *Isg-56* is regulated by *Socs-1*, we transfected a mouse macrophage cell line (RAW 264.7) with siRNA targeting *Socs-1* for 24 hr and infected these cells for an additional 24 hr with WNV (MOI = 0.1), followed by qPCR analysis. We found that *Socs-1* was slightly reduced following siRNA transfection in WNV-infected mouse RAW 264.7 cells (Fig. 5D) that was coupled to increased *Isg-56* (Fig. 5E) and *Tlr7* (Fig. 5F) expression. These results indicate that SOCS-1 signaling down-regulates *Tlr7* and *Isg-56* expression in mice. Since SOCS-1 associates with TLR8 directly (Fig. 5C) in mice, SOCS-1 may couple with TLR8 to inhibit the expression of *Tlr7* and subsequently its downstream signaling molecules, such as *Isg-56*, facilitating WNV infection in mice (Fig. 6).

Discussion

Human and mouse *Tlr7* and *Tlr8* share a high degree of structural and phylogenetic similarity, and are located only 70 kb apart on the same X chromosome (17, 24). Functionally, both human and mouse TLR7, and human TLR8 recognize viral ssRNA motifs. However, mouse TLR8 does not recognize viral ssRNA, which led to the belief that TLR8 may be non-functional in mouse in terms of sensing viral ssRNAs (16). It has since been suggested that mouse TLR8 recognizes DNA motifs of vaccinia virus (21) which however, was contradicted by another report (20). It has also been suggested that mouse TLR8 can recognize a combination of imidazoquinoline and poly-T oligodeoxynucleotides (22), however the natural ligand for mTLR8 still remains unknown. Our research group and others have demonstrated that mice deficient in TLR8 (*Tlr8*$^{-/-}$) overexpress *Tlr7* and manifest systemic autoimmunity due to development of a subset of B cells that produce anti-small nuclear ribonucleoproteins (snRNPs), anti-ribonucleoproteins (RNPs), and anti-DNA

antibodies (24-26, 59). On the other hand, transgenic mice that overexpress human TLR8 result in down-regulated mouse *Tlr7* expression (15). Based on these reports, it can be speculated that TLR8 in mice might have multiple functions to regulate immunity other than serving as a PRR. We previously reported that TLR7 plays an important role in the recognition and mitigation of WNV infection in mice (4). However, the role of mouse TLR8 during WNV pathogenesis has not been previously studied.

Defective *Tlr7* and type I *Ifn* genes are contributing factors to not only WNV susceptibility, but to enhanced WNV-induced disease (4, 60, 61). In the current report, we found that TLR8 deficiency in mice induced a strong antiviral immune response, which facilitated efficient control of viral burden and increased survival of mice after lethal WNV challenge. In line with previous reports that showed TLR8 negatively regulated TLR7 expression in mouse dendritic cells (24, 25), *Tlr8*$^{-/-}$ mice had increased gene expression of *Tlr7* in multiple tissues compared to WT controls, which was further amplified following WNV infection. While the mechanism by which increased *Tlr7* expression in the absence of viral infection was not further explored in this study, it has been suggested that deficiency in TLR signaling could be compensated for by other PRRs (62). Due to their close loci proximity and redundancy in pattern recognition (17, 63), TLR7 signaling may over-compensate for a loss of TLR8, as the reciprocal has been identified in TLR7 deficiency (64). Yet, in the context of viral infection, it may be possible that TLR8 directly or indirectly represses *Tlr7* transcription in mice. Based on the evidence that TLR8 co-precipitates with SOCS-1, and knockdown of *Socs-1* by siRNA leads to increased *Tlr7* transcription in WNV-infected RAW 264.7 cells, we may conclude that TLR8 couples to SOCS-1 to suppress the expression of *Tlr7* and its downstream signaling during WNV infection in mice. However, we cannot exclude the possibility that expression of *Tlr7* may be also indirectly enhanced by type I IFN responses induced by other PRRs, such as RIG-I and MDA5, in response to WNV infection (9). While we only measured inactive IRF-7 expression, active IRF-7-p has been described to act as a master transcription factor for IFNα (65, 66), which regulates the induction of *Isg-56* and *Tlr7* and thus, requires further study (67, 68). Furthermore, there was an overall increase in expression levels of TLR7, IRF-7, and ISG-56 in *Tlr8*$^{-/-}$ mice, in particular within primary neurons; therefore, involvement of multiple regulatory pathways may contribute to hyperactive antiviral immunity to control viral infection. In line with this, it has been described that functional polymorphisms in the human *Tlr8* gene may predispose individuals to differential viral susceptibility (14, 69-72). For instance, TLR8C-A haplotypes are associated with dengue fever susceptibility, while TLR8G-G haplotypes are associated with dengue hemorrhagic fever susceptibility (71) and truncated *Tlr8* protects against HIV, as rapid decay of *Tlr8* mRNA results in induced TNF-α signaling (70). Therefore, TLR8 may function to suppress antiviral immunity through negative regulation of TLR7 signaling.

ISG-56 (IFIT-1), along with other IFIT family members including ISG-54 (IFIT-2) and ISG-49 (IFIT-3) protect neurons from WNV infection (33, 34, 73). These molecules are enhanced by type I IFNs during viral infection (9, 56) and function by binding to the 5'-PPP end of viral RNA, mRNA, or to the translation initiation factor eIF-3, to inhibit the initiation of viral/host protein translation (33, 67, 74). WNV-infected *Tlr8*$^{-/-}$ mice expressed higher levels of type I IFNs and *Isg-56* in various tissues compared to WT controls. Moreover, increased expression of *Isg-54* (IFIT-2) and *Isg-49* (IFIT-3) were also observed in WNV-

infected *Tlr8*$^{-/-}$ mice neurons, suggesting a vast array of enhanced antiviral immunity. Consistent with the previous report that IFITs are vital antiviral proteins that work in concert to control viral infection within the CNS (75), we further verified the importance of *Isg-56* during WNV infection in *Tlr8*$^{-/-}$ mice by knocking down its expression, which resulted in an increased WNV-induced neuronal apoptosis mediated by *Bax,* highlighting an important role for ISG-56 during WNV-induced neuronal death.

Tissue and cellular tropism of WNV is regulated by antiviral gene localization (56, 76) and IFIT molecules play a crucial role in controlling viral spread within neurons (33). Additionally, the cerebellum and choroid plexus express *Isg-56* following WNV infection (33), and IFNβ treatment induces a higher expression of *Isg-56* in cerebellar cells (56). In line with this, we observed a significant increase of *Isg-56* only within the spinal cord and cerebellar regions of *Tlr8*$^{-/-}$ mice brains, together with reduced morbidity, suggesting neuropathogenesis of WNV may be limited by antiviral control only within these regions of the CNS. Overexpression of *Tlr7* in the CNS has been linked to the induction of IL-6 dependent dendrite retraction (64) and leads to cell death by induction of a CNS-specific TIR adaptor protein called Sterile alpha and HEAT/Armadillo motif (SARM) (77). Yet in the presence of WNV infection, SARM is necessary to reduce WNV burden and prevent cell death, as *Sarm*$^{-/-}$ mice are susceptible to WNV infection (78). In addition, TLR7 agonists, imiquimod and ssRNA, have been described to induce neuronal cell death (79). However, there are no phenotypic or behavioral defects observed in naïve *Tlr8*$^{-/-}$ mice, and increased percent of survival and reduced TUNEL signals observed within *Tlr8*$^{-/-}$ mice brains following lethal WNV challenge, suggest that increased TLR7 does not cause any apparent neuronal damage in our experimental conditions. Furthermore, the expression of TLR7 observed in the brains of *Tlr8*$^{-/-}$ mice is relatively mild, which suggests that only dramatically increased expression/signaling by TLR7 may lead to neuronal damage.

Suppressor of cytokine signaling (SOCS)-1, a negative regulator of IFN signaling, can be induced following viral challenge (29, 80-82). SOCS-1 suppresses a multitude of signaling molecules, such as the Mal adaptor protein in TLR4 signaling (83), IRAK-4 (84), TRAF6 (85), type I IFNs (30, 58), JAKs (86) and transcriptional promoters including STAT-1 (58, 87), IRF7 (88) and p53 (89). Importantly, *Socs-1* knockdown in Japanese encephalitis virus (JEV)-infected macrophages resulted in reduced viral load and increased ISGs, suggesting that SOCS-1 may directly regulate expression of ISGs (90). Since *Tlr8*$^{-/-}$ mice had a hyperactive IFN response and reduced *Socs-1*, we hypothesized that TLR8 signaling may regulate *Socs-1* expression. It has been reported that TLR7/8 signaling induces the expression of *Socs-1* in HEK293 cells, yet these studies did not rule out if this signaling is dependent on TLR7 or TLR8 alone, or an effect of combined TLR7 and TLR8 ligation (91). In our report, we demonstrated that SOCS-1 partnered with TLR8, but not TLR7, suggesting SOCS-1 utilizes TLR8 as an adaptor molecule for its regulation. This interaction is possible as there are 13 phospho-tyrosine residues located on the cytoplasmic domain of TLR8, but not on TLR7 (92), which provides ample docking sites for the SH2 regions of SOCS-1 to bind to TLR8. SOCS proteins function to directly associate and inhibit adaptor proteins and their signaling pathways via protein degradation (83). However, we observed a stable interaction between TLR8 and SOCS-1 24 hr post stimulation in Neuro-2a cells, suggesting a non-canonical role for TLR8 SOCS-1 regulation that requires further investigation.

In conclusion, TLR8 couples with SOCS-1 to exacerbate neuroinvasive WNV infection in mice, by negative regulation of TLR7-mediated antiviral immunity in mice. The identification of a novel role for SOCS-1 in TLR8-mediated immune regulation may have broad implications in understanding antiviral immunity in both mice and humans. Although human TLR8 regulation of TLR7 with SOCS-1 was not studied in this manuscript, the therapeutic potential of inhibiting the TLR8 pathway may provide an alternative antiviral strategy to combat WNV infection in humans, which requires further investigation.

Supplementary Material

Refer to Web version on PubMed Central for supplementary material.

Acknowledgments

We thank Dr. John F. Anderson at the Connecticut Agricultural Experiment Station for providing the WNV isolate (CT2741), USM animal facility for excellent care of our mice, and Mississippi INBRE for the use of the facility's equipment.

Financial Support. This work was supported in part by The University of Southern Mississippi Start-up fund and The Aubrey Keith Lucas and Ella Ginn Lucas Endowment for Faculty Excellence award (F.B.), National Institute of Allergy and Infectious Diseases of the National Institutes of Health R15AI113706 (F.B), and the Wilson Research Foundation.

References

1. Reisen WK. Ecology of West Nile virus in North America. Viruses. 2013; 5:2079–2105. [PubMed: 24008376]
2. Lim SM, Koraka P, Osterhaus AD, Martina BE. West Nile virus: immunity and pathogenesis. Viruses. 2011; 3:811–828. [PubMed: 21994755]
3. Wang T, Town T, Alexopoulou L, Anderson JF, Fikrig E, Flavell RA. Toll-like receptor 3 mediates West Nile virus entry into the brain causing lethal encephalitis. Nature medicine. 2004; 10:1366–1373.
4. Town T, Bai F, Wang T, Kaplan AT, Qian F, Montgomery RR, Anderson JF, Flavell RA, Fikrig E. Toll-like receptor 7 mitigates lethal West Nile encephalitis via interleukin 23-dependent immune cell infiltration and homing. Immunity. 2009; 30:242–253. [PubMed: 19200759]
5. Szretter KJ, Daffis S, Patel J, Suthar MS, Klein RS, Gale M Jr. Diamond MS. The innate immune adaptor molecule MyD88 restricts West Nile virus replication and spread in neurons of the central nervous system. Journal of virology. 2010; 84:12125–12138. [PubMed: 20881045]
6. Kawai T, Akira S. Antiviral signaling through pattern recognition receptors. J Biochem. 2007; 141:137–145. [PubMed: 17190786]
7. Xie G, Welte T, Wang J, Whiteman MC, Wicker JA, Saxena V, Cong Y, Barrett AD, Wang T. A West Nile virus NS4B-P38G mutant strain induces adaptive immunity via TLR7-MyD88-dependent and independent signaling pathways. Vaccine. 2013; 31:4143–4151. [PubMed: 23845800]
8. Xia J, Winkelmann ER, Gorder SR, Mason PW, Milligan GN. TLR3- and MyD88-dependent signaling differentially influences the development of West Nile virus-specific B cell responses in mice following immunization with RepliVAX WN, a single-cycle flavivirus vaccine candidate. Journal of virology. 2013; 87:12090–12101. [PubMed: 23986602]
9. Fredericksen BL, Keller BC, Fornek J, Katze MG, Gale M Jr. Establishment and maintenance of the innate antiviral response to West Nile Virus involves both RIG-I and MDA5 signaling through IPS-1. Journal of virology. 2008; 82:609–616. [PubMed: 17977974]
10. Schoggins JW, Rice CM. Interferon-stimulated genes and their antiviral effector functions. Current opinion in virology. 2011; 1:519–525. [PubMed: 22328912]

11. Pine SO, McElrath MJ, Bochud PY. Polymorphisms in toll-like receptor 4 and toll-like receptor 9 influence viral load in a seroincident cohort of HIV-1-infected individuals. AIDS. 2009; 23:2387–2395. [PubMed: 19855253]
12. Oh DY, Baumann K, Hamouda O, Eckert JK, Neumann K, Kucherer C, Bartmeyer B, Poggensee G, Oh N, Pruss A, Jessen H, Schumann RR. A frequent functional toll-like receptor 7 polymorphism is associated with accelerated HIV-1 disease progression. AIDS. 2009; 23:297–307. [PubMed: 19114863]
13. Bochud PY, Magaret AS, Koelle DM, Aderem A, Wald A. Polymorphisms in TLR2 are associated with increased viral shedding and lesional rate in patients with genital herpes simplex virus Type 2 infection. The Journal of infectious diseases. 2007; 196:505–509. [PubMed: 17624834]
14. Hise AG, Traylor Z, Hall NB, Sutherland LJ, Dahir S, Ermler ME, Muiruri S, Muchiri EM, Kazura JW, LaBeaud AD, King CH, Stein CM. Association of symptoms and severity of rift valley fever with genetic polymorphisms in human innate immune pathways. PLoS neglected tropical diseases. 2015; 9:e0003584. [PubMed: 25756647]
15. Guiducci C, Gong M, Cepika AM, Xu Z, Tripodo C, Bennett L, Crain C, Quartier P, Cush JJ, Pascual V, Coffman RL, Barrat FJ. RNA recognition by human TLR8 can lead to autoimmune inflammation. The Journal of experimental medicine. 2013; 210:2903–2919. [PubMed: 24277153]
16. Forsbach A, Nemorin JG, Montino C, Muller C, Samulowitz U, Vicari AP, Jurk M, Mutwiri GK, Krieg AM, Lipford GB, Vollmer J. Identification of RNA sequence motifs stimulating sequence-specific TLR8-dependent immune responses. J Immunol. 2008; 180:3729–3738. [PubMed: 18322178]
17. Heil F, Hemmi H, Hochrein H, Ampenberger F, Kirschning C, Akira S, Lipford G, Wagner H, Bauer S. Species-specific recognition of single-stranded RNA via toll-like receptor 7 and 8. Science. 2004; 303:1526–1529. [PubMed: 14976262]
18. Ma Y, Haynes RL, Sidman RL, Vartanian T. TLR8: an innate immune receptor in brain, neurons and axons. Cell Cycle. 2007; 6:2859–2868. [PubMed: 18000403]
19. Liu J, Xu C, Hsu LC, Luo Y, Xiang R, Chuang TH. A five-amino-acid motif in the undefined region of the TLR8 ectodomain is required for species-specific ligand recognition. Mol Immunol. 2010; 47:1083–1090. [PubMed: 20004021]
20. Bauer S, Bathke B, Lauterbach H, Patzold J, Kassub R, Luber CA, Schlatter B, Hamm S, Chaplin P, Suter M, Hochrein H. A major role for TLR8 in the recognition of vaccinia viral DNA by murine pDC? Proceedings of the National Academy of Sciences of the United States of America. 2010; 107:E139. author reply E140. [PubMed: 20679190]
21. Martinez J, Huang X, Yang Y. Toll-like receptor 8-mediated activation of murine plasmacytoid dendritic cells by vaccinia viral DNA. Proceedings of the National Academy of Sciences of the United States of America. 2010; 107:6442–6447. [PubMed: 20308556]
22. Gorden KK, Qiu XX, Binsfeld CC, Vasilakos JP, Alkan SS. Cutting edge: activation of murine TLR8 by a combination of imidazoquinoline immune response modifiers and polyT oligodeoxynucleotides. J Immunol. 2006; 177:6584–6587. [PubMed: 17082568]
23. Li T, He X, Jia H, Chen G, Zeng S, Fang Y, Jin Q, Jing Z. Molecular cloning and functional characterization of murine tolllike receptor 8. Molecular medicine reports. 2016; 13:1119–1126. [PubMed: 26676274]
24. Demaria O, Pagni PP, Traub S, de Gassart A, Branzk N, Murphy AJ, Valenzuela DM, Yancopoulos GD, Flavell RA, Alexopoulou L. TLR8 deficiency leads to autoimmunity in mice. J Clin Invest. 2010; 120:3651–3662. [PubMed: 20811154]
25. Desnues B, Macedo AB, Roussel-Queval A, Bonnardel J, Henri S, Demaria O, Alexopoulou L. TLR8 on dendritic cells and TLR9 on B cells restrain TLR7-mediated spontaneous autoimmunity in C57BL/6 mice. Proceedings of the National Academy of Sciences of the United States of America. 2014; 111:1497–1502. [PubMed: 24474776]
26. Tran NL, Manzin-Lorenzi C, Santiago-Raber ML. Toll-like receptor 8 deletion accelerates autoimmunity in a mouse model of lupus through a Toll-like receptor 7-dependent mechanism. Immunology. 2015; 145:60–70. [PubMed: 25424423]
27. Yoshimura A, Ohishi HM, Aki D, Hanada T. Regulation of TLR signaling and inflammation by SOCS family proteins. Journal of leukocyte biology. 2004; 75:422–427. [PubMed: 14726494]

28. Krebs DL, Hilton DJ. SOCS proteins: negative regulators of cytokine signaling. Stem Cells. 2001; 19:378–387. [PubMed: 11553846]
29. Mansfield KL, Johnson N, Cosby SL, Solomon T, Fooks AR. Transcriptional upregulation of SOCS 1 and suppressors of cytokine signaling 3 mRNA in the absence of suppressors of cytokine signaling 2 mRNA after infection with West Nile virus or tick-borne encephalitis virus. Vector Borne Zoonotic Dis. 2010; 10:649–653. [PubMed: 20854017]
30. Song MM, Shuai K. The suppressor of cytokine signaling (SOCS) 1 and SOCS3 but not SOCS2 proteins inhibit interferon-mediated antiviral and antiproliferative activities. The Journal of biological chemistry. 1998; 273:35056–35062. [PubMed: 9857039]
31. Sen GC, Sarkar SN. The interferon-stimulated genes: targets of direct signaling by interferons, double-stranded RNA, and viruses. Current topics in microbiology and immunology. 2007; 316:233–250. [PubMed: 17969451]
32. Fensterl V, Sen GC. The ISG56/IFIT1 gene family. Journal of interferon & cytokine research : the official journal of the International Society for Interferon and Cytokine Research. 2011; 31:71–78.
33. Wacher C, Muller M, Hofer MJ, Getts DR, Zabaras R, Ousman SS, Terenzi F, Sen GC, King NJ, Campbell IL. Coordinated regulation and widespread cellular expression of interferon-stimulated genes (ISG) ISG-49, ISG-54, and ISG-56 in the central nervous system after infection with distinct viruses. Journal of virology. 2007; 81:860–871. [PubMed: 17079283]
34. Szretter KJ, Daniels BP, Cho H, Gainey MD, Yokoyama WM, Gale M Jr. Virgin HW, Klein RS, Sen GC, Diamond MS. 2′-O methylation of the viral mRNA cap by West Nile virus evades ifit1-dependent and -independent mechanisms of host restriction in vivo. PLoS pathogens. 2012; 8:e1002698. [PubMed: 22589727]
35. Paul AM, Shi Y, Acharya D, Douglas JR, Cooley A, Anderson JF, Huang F, Bai F. Delivery of antiviral small interfering RNA with gold nanoparticles inhibits dengue virus infection in vitro. The Journal of general virology. 2014; 95:1712–1722. [PubMed: 24828333]
36. Gardner J, Anraku I, Le TT, Larcher T, Major L, Roques P, Schroder WA, Higgs S, Suhrbier A. Chikungunya virus arthritis in adult wild-type mice. Journal of virology. 2010; 84:8021–8032. [PubMed: 20519386]
37. Teo TH, Lum FM, Claser C, Lulla V, Lulla A, Merits A, Renia L, Ng LF. A pathogenic role for CD4+ T cells during Chikungunya virus infection in mice. J Immunol. 2013; 190:259–269. [PubMed: 23209328]
38. Teng TS, Foo SS, Simamarta D, Lum FM, Teo TH, Lulla A, Yeo NK, Koh EG, Chow A, Leo YS, Merits A, Chin KC, Ng LF. Viperin restricts chikungunya virus replication and pathology. J Clin Invest. 2012; 122:4447–4460. [PubMed: 23160199]
39. Lutz MB, Kukutsch N, Ogilvie AL, Rossner S, Koch F, Romani N, Schuler G. An advanced culture method for generating large quantities of highly pure dendritic cells from mouse bone marrow. J Immunol Methods. 1999; 223:77–92. [PubMed: 10037236]
40. Eide L, McMurray CT. Culture of adult mouse neurons. Biotechniques. 2005; 38:99–104. [PubMed: 15679091]
41. Bai F, Town T, Qian F, Wang P, Kamanaka M, Connolly TM, Gate D, Montgomery RR, Flavell RA, Fikrig E. IL-10 signaling blockade controls murine West Nile virus infection. PLoS pathogens. 2009; 5:e1000610. [PubMed: 19816558]
42. Bai F, Wang T, Pal U, Bao F, Gould LH, Fikrig E. Use of RNA interference to prevent lethal murine west nile virus infection. The Journal of infectious diseases. 2005; 191:1148–1154. [PubMed: 15747251]
43. Daffis S, Samuel MA, Keller BC, Gale M Jr. Diamond MS. Cell-specific IRF-3 responses protect against West Nile virus infection by interferon-dependent and -independent mechanisms. PLoS pathogens. 2007; 3:e106. [PubMed: 17676997]
44. Fensterl V, White CL, Yamashita M, Sen GC. Novel characteristics of the function and induction of murine p56 family proteins. Journal of virology. 2008; 82:11045–11053. [PubMed: 18768971]
45. Ueki K, Kondo T, Kahn CR. Suppressor of cytokine signaling 1 (SOCS-1) and SOCS-3 cause insulin resistance through inhibition of tyrosine phosphorylation of insulin receptor substrate proteins by discrete mechanisms. Molecular and cellular biology. 2004; 24:5434–5446. [PubMed: 15169905]

46. Schneider CA, Rasband WS, Eliceiri KW. NIH Image to ImageJ: 25 years of image analysis. Nature methods. 2012; 9:671–675. [PubMed: 22930834]
47. Rieger AM, Nelson KL, Konowalchuk JD, Barreda DR. Modified annexin V/propidium iodide apoptosis assay for accurate assessment of cell death. Journal of visualized experiments : JoVE. 2011
48. Daffis S, Samuel MA, Suthar MS, Keller BC, Gale M Jr. Diamond MS. Interferon regulatory factor IRF-7 induces the antiviral alpha interferon response and protects against lethal West Nile virus infection. Journal of virology. 2008; 82:8465–8475. [PubMed: 18562536]
49. Bourne N, Scholle F, Silva MC, Rossi SL, Dewsbury N, Judy B, De Aguiar JB, Leon MA, Estes DM, Fayzulin R, Mason PW. Early production of type I interferon during West Nile virus infection: role for lymphoid tissues in IRF3-independent interferon production. Journal of virology. 2007; 81:9100–9108. [PubMed: 17567689]
50. Parquet MC, Kumatori A, Hasebe F, Morita K, Igarashi A. West Nile virus-induced bax-dependent apoptosis. FEBS letters. 2001; 500:17–24. [PubMed: 11434919]
51. Yang MR, Lee SR, Oh W, Lee EW, Yeh JY, Nah JJ, Joo YS, Shin J, Lee HW, Pyo S, Song J. West Nile virus capsid protein induces p53-mediated apoptosis via the sequestration of HDM2 to the nucleolus. Cellular microbiology. 2008; 10:165–176. [PubMed: 17697133]
52. Samuel MA, Diamond MS. Alpha/beta interferon protects against lethal West Nile virus infection by restricting cellular tropism and enhancing neuronal survival. Journal of virology. 2005; 79:13350–13361. [PubMed: 16227257]
53. Lim SM, Koraka P, van Boheemen S, Roose JM, Jaarsma D, van de Vijver DA, Osterhaus AD, Martina BE. Characterization of the mouse neuroinvasiveness of selected European strains of West Nile virus. PloS one. 2013; 8:e74575. [PubMed: 24058590]
54. Shrestha B, Diamond MS. Role of CD8+ T cells in control of West Nile virus infection. Journal of virology. 2004; 78:8312–8321. [PubMed: 15254203]
55. Omalu BI, Shakir AA, Wang G, Lipkin WI, Wiley CA. Fatal fulminant pan-meningo-polioencephalitis due to West Nile virus. Brain Pathol. 2003; 13:465–472. [PubMed: 14655752]
56. Cho H, Proll SC, Szretter KJ, Katze MG, Gale M Jr. Diamond MS. Differential innate immune response programs in neuronal subtypes determine susceptibility to infection in the brain by positive-stranded RNA viruses. Nature medicine. 2013; 19:458–464.
57. Sandhu TS, Sidhu DS, Dhillon MS. Antigenic distribution of west nile virus in various organs of wildly infected american crows (corvus brachyrhynchos). Journal of global infectious diseases. 2011; 3:138–142. [PubMed: 21731300]
58. Prele CM, Woodward EA, Bisley J, Keith-Magee A, Nicholson SE, Hart PH. SOCS1 regulates the IFN but not NFkappaB pathway in TLR-stimulated human monocytes and macrophages. J Immunol. 2008; 181:8018–8026. [PubMed: 19017994]
59. Tran NL, Manzin-Lorenzi C, Santiago-Raber ML. TLR8 deletion accelerates autoimmunity in a mouse model of lupus through a TLR7-dependent mechanism. Immunology. 2014
60. Qian F, Wang X, Zhang L, Lin A, Zhao H, Fikrig E, Montgomery RR. Impaired interferon signaling in dendritic cells from older donors infected in vitro with West Nile virus. The Journal of infectious diseases. 2011; 203:1415–1424. [PubMed: 21398396]
61. Xie G, Luo H, Pang L, Peng BH, Winkelmann E, McGruder B, Hesse J, Whiteman M, Campbell G, Milligan GN, Cong Y, Barrett AD, Wang T. Dysregulation of Toll-Like Receptor 7 Compromises Innate and Adaptive T Cell Responses and Host Resistance to an Attenuated West Nile Virus Infection in Old Mice. Journal of virology. 2015; 90:1333–1344. [PubMed: 26581984]
62. Kawai T, Akira S. Toll-like receptors and their crosstalk with other innate receptors in infection and immunity. Immunity. 2011; 34:637–650. [PubMed: 21616434]
63. Hornung V, Barchet W, Schlee M, Hartmann G. RNA recognition via TLR7 and TLR8. Handbook of experimental pharmacology. 2008:71–86. [PubMed: 18071655]
64. Liu HY, Hong YF, Huang CM, Chen CY, Huang TN, Hsueh YP. TLR7 negatively regulates dendrite outgrowth through the Myd88-c-Fos-IL-6 pathway. The Journal of neuroscience : the official journal of the Society for Neuroscience. 2013; 33:11479–11493. [PubMed: 23843519]

65. Wang Y, Yan S, Yang B, Wang Y, Zhou H, Lian Q, Sun B. TRIM35 negatively regulates TLR7- and TLR9-mediated type I interferon production by targeting IRF7. FEBS letters. 2015; 589:1322–1330. [PubMed: 25907537]

66. Sato M, Suemori H, Hata N, Asagiri M, Ogasawara K, Nakao K, Nakaya T, Katsuki M, Noguchi S, Tanaka N, Taniguchi T. Distinct and essential roles of transcription factors IRF-3 and IRF-7 in response to viruses for IFN-alpha/beta gene induction. Immunity. 2000; 13:539–548. [PubMed: 11070172]

67. Zhou X, Michal JJ, Zhang L, Ding B, Lunney JK, Liu B, Jiang Z. Interferon induced IFIT family genes in host antiviral defense. International journal of biological sciences. 2013; 9:200–208. [PubMed: 23459883]

68. Siren J, Pirhonen J, Julkunen I, Matikainen S. IFN-alpha regulates TLR-dependent gene expression of IFN-alpha, IFN-beta, IL-28, and IL-29. J Immunol. 2005; 174:1932–1937. [PubMed: 15699120]

69. Wang CH, Eng HL, Lin KH, Liu HC, Chang CH, Lin TM. Functional polymorphisms of TLR8 are associated with hepatitis C virus infection. Immunology. 2014; 141:540–548. [PubMed: 24205871]

70. Oh DY, Taube S, Hamouda O, Kucherer C, Poggensee G, Jessen H, Eckert JK, Neumann K, Storek A, Pouliot M, Borgeat P, Oh N, Schreier E, Pruss A, Hattermann K, Schumann RR. A functional toll-like receptor 8 variant is associated with HIV disease restriction. The Journal of infectious diseases. 2008; 198:701–709. [PubMed: 18605904]

71. Alagarasu K, Bachal RV, Memane RS, Shah PS, Cecilia D. Polymorphisms in RNA sensing toll like receptor genes and its association with clinical outcomes of dengue virus infection. Immunobiology. 2015; 220:164–168. [PubMed: 25446400]

72. Wang CH, Eng HL, Lin KH, Chang CH, Hsieh CA, Lin YL, Lin TM. TLR7 and TLR8 gene variations and susceptibility to hepatitis C virus infection. PloS one. 2011; 6:e26235. [PubMed: 22022576]

73. Cho H, Shrestha B, Sen GC, Diamond MS. A role for Ifit2 in restricting West Nile virus infection in the brain. Journal of virology. 2013; 87:8363–8371. [PubMed: 23740986]

74. Fensterl V, Sen GC. Interferon-induced Ifit proteins: Their role in viral pathogenesis. Journal of virology. 2014

75. Lazear HM, Diamond MS. New insights into innate immune restriction of West Nile virus infection. Current opinion in virology. 2014; 11C:1–6.

76. Suthar MS, Brassil MM, Blahnik G, McMillan A, Ramos HJ, Proll SC, Belisle SE, Katze MG, Gale M Jr. A systems biology approach reveals that tissue tropism to West Nile virus is regulated by antiviral genes and innate immune cellular processes. PLoS pathogens. 2013; 9:e1003168. [PubMed: 23544010]

77. Mukherjee P, Winkler CW, Taylor KG, Woods TA, Nair V, Khan BA, Peterson KE. SARM1, Not MyD88, Mediates TLR7/TLR9-Induced Apoptosis in Neurons. J Immunol. 2015; 195:4913–4921. [PubMed: 26423149]

78. Szretter KJ, Samuel MA, Gilfillan S, Fuchs A, Colonna M, Diamond MS. The immune adaptor molecule SARM modulates tumor necrosis factor alpha production and microglia activation in the brainstem and restricts West Nile Virus pathogenesis. Journal of virology. 2009; 83:9329–9338. [PubMed: 19587044]

79. Lehmann SM, Rosenberger K, Kruger C, Habbel P, Derkow K, Kaul D, Rybak A, Brandt C, Schott E, Wulczyn FG, Lehnardt S. Extracellularly delivered single-stranded viral RNA causes neurodegeneration dependent on TLR7. J Immunol. 2012; 189:1448–1458. [PubMed: 22745379]

80. Inagaki-Ohara K, Kondo T, Ito M, Yoshimura A. SOCS, inflammation, and cancer. Jak-Stat. 2013; 2:e24053. [PubMed: 24069550]

81. Kazi JU, Kabir NN, Flores-Morales A, Ronnstrand L. SOCS proteins in regulation of receptor tyrosine kinase signaling. Cellular and molecular life sciences : CMLS. 2014; 71:3297–3310. [PubMed: 24705897]

82. Ahmed CM, Larkin J 3rd, Johnson HM. SOCS1 Mimetics and Antagonists: A Complementary Approach to Positive and Negative Regulation of Immune Function. Frontiers in immunology. 2015; 6:183. [PubMed: 25954276]

83. Mansell A, Smith R, Doyle SL, Gray P, Fenner JE, Crack PJ, Nicholson SE, Hilton DJ, O'Neill LA, Hertzog PJ. Suppressor of cytokine signaling 1 negatively regulates Toll-like receptor signaling by mediating Mal degradation. Nature immunology. 2006; 7:148–155. [PubMed: 16415872]
84. Trinath J, Holla S, Mahadik K, Prakhar P, Singh V, Balaji KN. The WNT signaling pathway contributes to dectin-1-dependent inhibition of Toll-like receptor-induced inflammatory signature. Molecular and cellular biology. 2014; 34:4301–4314. [PubMed: 25246634]
85. Zhou X, Liu Z, Cheng X, Zheng Y, Zeng F, He Y. Socs1 and Socs3 degrades Traf6 via polyubiquitination in LPS-induced acute necrotizing pancreatitis. Cell death & disease. 2015; 6:e2012. [PubMed: 26633718]
86. Tamiya T, Kashiwagi I, Takahashi R, Yasukawa H, Yoshimura A. Suppressors of cytokine signaling (SOCS) proteins and JAK/STAT pathways: regulation of T-cell inflammation by SOCS1 and SOCS3. Arteriosclerosis, thrombosis, and vascular biology. 2011; 31:980–985.
87. Kimura A, Naka T, Muta T, Takeuchi O, Akira S, Kawase I, Kishimoto T. Suppressor of cytokine signaling-1 selectively inhibits LPS-induced IL-6 production by regulating JAK-STAT. Proceedings of the National Academy of Sciences of the United States of America. 2005; 102:17089–17094. [PubMed: 16287972]
88. Dai X, Sayama K, Yamasaki K, Tohyama M, Shirakata Y, Hanakawa Y, Tokumaru S, Yahata Y, Yang L, Yoshimura A, Hashimoto K. SOCS1-negative feedback of STAT1 activation is a key pathway in the dsRNA-induced innate immune response of human keratinocytes. The Journal of investigative dermatology. 2006; 126:1574–1581. [PubMed: 16628196]
89. Mallette FA, Calabrese V, Ilangumaran S, Ferbeyre G. SOCS1, a novel interaction partner of p53 controlling oncogene-induced senescence. Aging. 2010; 2:445–452. [PubMed: 20622265]
90. Kundu K, Dutta K, Nazmi A, Basu A. Japanese encephalitis virus infection modulates the expression of suppressors of cytokine signaling (SOCS) in macrophages: implications for the hosts' innate immune response. Cellular immunology. 2013; 285:100–110. [PubMed: 24140964]
91. Hildebrand D, Walker P, Dalpke A, Heeg K, Kubatzky KF. Pasteurella multocida Toxin-induced Pim-1 expression disrupts suppressor of cytokine signalling (SOCS)-1 activity. Cellular microbiology. 2010; 12:1732–1745. [PubMed: 20633028]
92. Chattopadhyay S, Sen GC. Tyrosine phosphorylation in Toll-like receptor signaling. Cytokine & growth factor reviews. 2014; 25:533–541. [PubMed: 25022196]

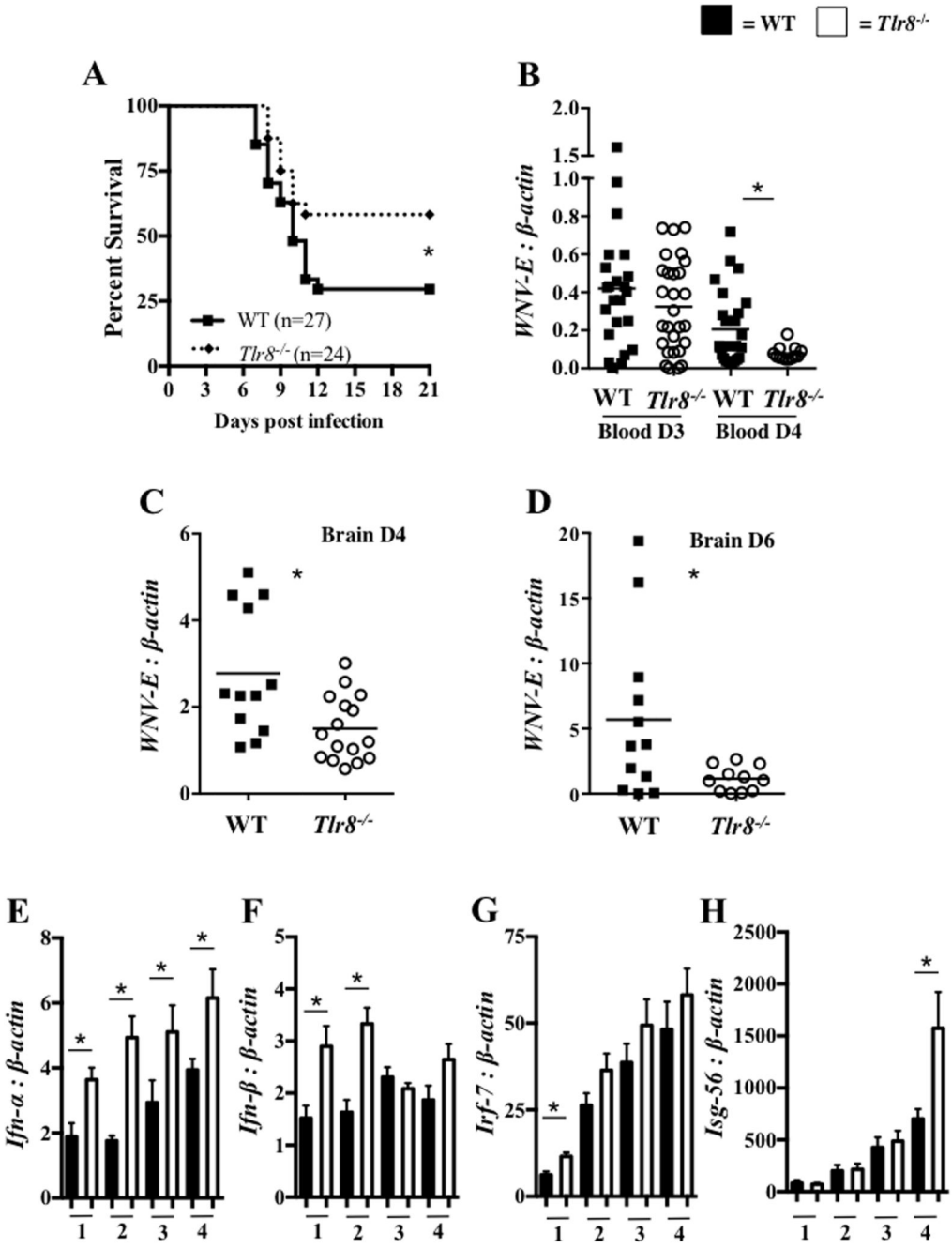

Figure 1. *Tlr8*$^{-/-}$ mice are resistant to lethal WNV infection

WT and *Tlr8*$^{-/-}$ mice were infected with 2000 PFU/mouse of WNV and monitored twice daily for mortality and morbidity for up to 21 days. **(A)** Survival analysis of WT and *Tlr8*$^{-/-}$ mice by Kaplan-Meier analysis. The ratio of *WNV-envelope (E)* to *β-actin* in blood **(B)** and brain samples at day 4 **(C)** and day 6 **(D)** p.i., collected from euthanized mice was determined by qPCR. The absolute gene copy ratio of *Ifn-α* **(E),** *Ifn-β* **(F),** *Irf-7* **(G)** and *Isg-56* **(H)** to *β-actin* were measured in blood samples by qPCR at indicated days p.i. (n = 5-8 per group). The survival data were analyzed using a Kaplan-Meier log-rank test (*

denotes $p < 0.05$). Gene expression data were analyzed using a two-tailed, Student's *t*-test (* denotes $p < 0.05 \pm 1$ SEM). All reported experiments were performed twice.

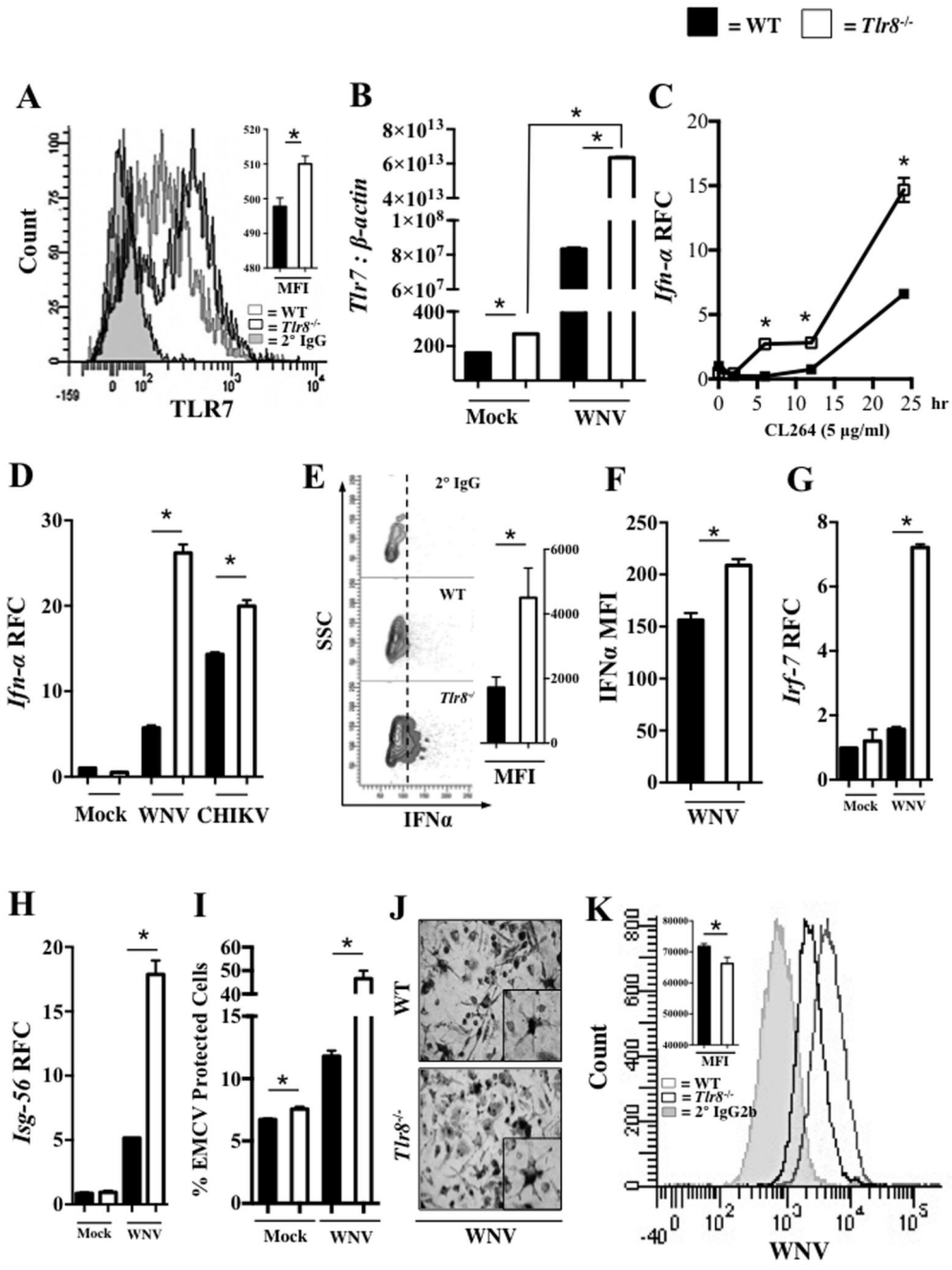

Figure 2. TLR8 signaling negatively regulates TLR7-mediated antiviral immunity

(A) Flow cytometric histograms and mean fluorescent intensity (MFI) analysis of TLR7 expression in blood collected from WNV-infected WT (grey outline), *Tlr8*$^{-/-}$ (black outline), and secondary only IgG isotype control (grey filled) mice (n = 6-8 per group) at day 1 p.i.. QPCR analysis for gene expression of **(B)** *Tlr7*, **(D)** *Ifn-α*, **(G)** *Irf-7,* and **(H)** *Isg-56* in WT and *Tlr8*$^{-/-}$ mice BMDCs infected *in vitro* with WNV or CHIKV (MOI = 5) for 24 hr. BMDCs from WT and *Tlr8*$^{-/-}$ mice were stimulated *in vitro* with the TLR7 ligand CL264 (5 μg/ml) for indicated time points and gene expression of *Ifn-α* **(C)** was measured by qPCR.

Flow cytometic analysis of IFN-α expression in BMDCs infected with WNV (MOI = 5) for 24 hr **(E)** and IFN-α production in the media **(F)** of WT and *Tlr8*$^{-/-}$ BMDCs infected with WNV (MOI = 5) for 24 hr. **(I)** IFN production in the culture media of WNV-infected WT and *Tlr8*$^{-/-}$ BMDCs were measured by an IFN-bioassay. **(J)** Immunocytochemistry images of BMDCs infected with WNV for 24 hr (400 × magnification, inset 900 × magnification). **(K)** Flow cytometric analysis of WNV-Envelope protein in BMDCs infected with WNV (MOI = 5) for 24hr. WT (grey outline), *Tlr8*$^{-/-}$ (black outline), and secondary only IgG2b isotype control (grey filled) mice. The gene expression profile of Figure 1B is represented as a mean unitless ratio of gene of interest to *β-actin* ± 1 SEM, while all remaining qPCR profiles were normalized to *β-actin* and were plotted as relative fold change (RFC). All qPCR assays were performed three times and were analyzed using a two-tailed, Student's *t*-test (* denotes $p < 0.05 \pm 1$ SEM, n = 3 per group). The IFN-bioassay and the flow cytometric analysis in blood was performed once, and the flow cytometric analysis in BMDCs (n = 3 per group) was performed twice, and analyzed using a two-tailed, Student's *t*-test (* denotes $p < 0.05 \pm 1$ SEM).

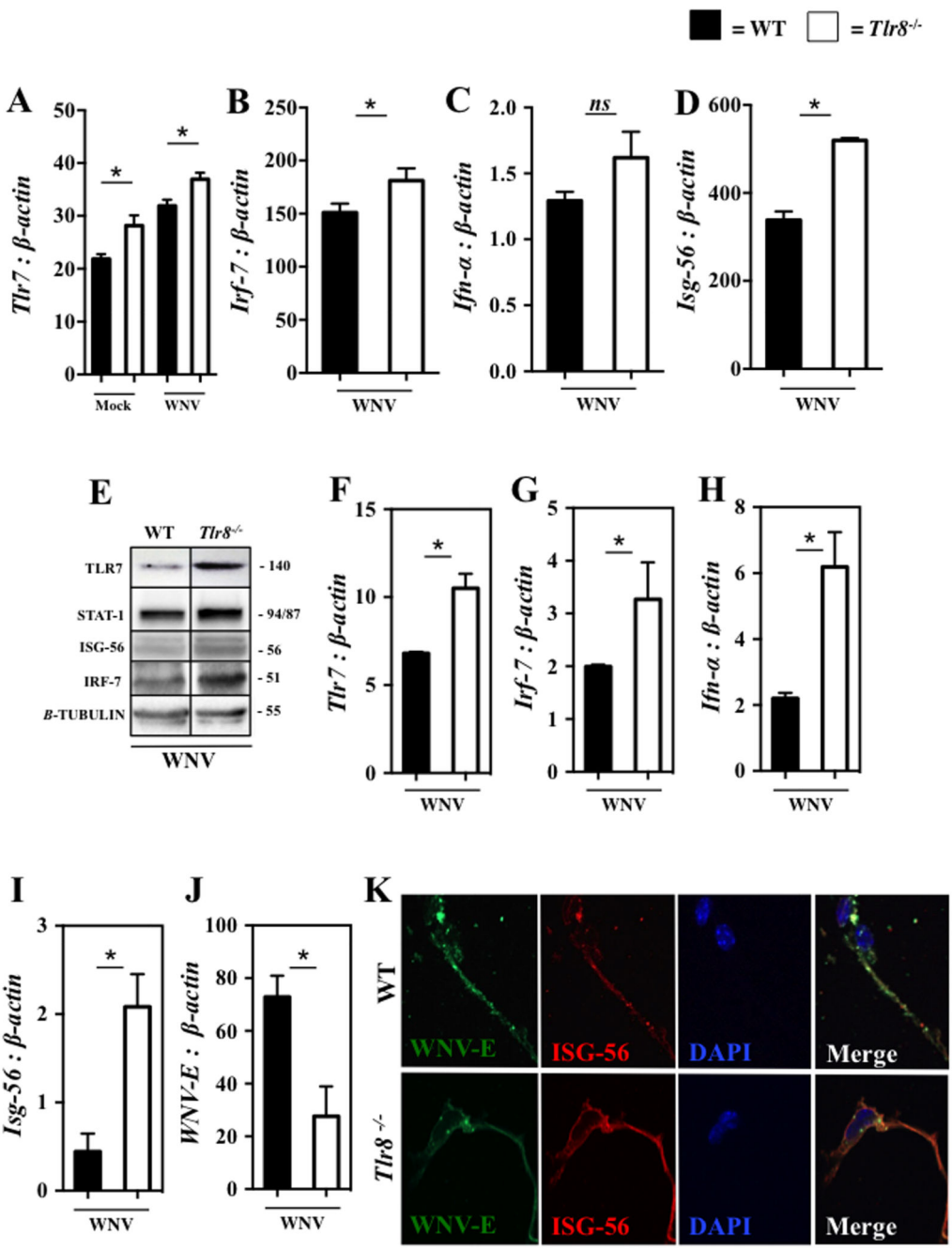

Figure 3. *Tlr8*$^{-/-}$ mice have increased antiviral immunity in CNS tissue

Gene expression analysis of *Tlr7* **(A)**, *Irf-7* **(B)**, *Ifn-α* **(C)**, *Isg-56* **(D)** to *β-actin* in whole brains from WNV-infected WT and *Tlr8*$^{-/-}$ mice at day 4 p.i. by qPCR (n = 6-8 per group). **(E)** Immunoblotting analysis of TLR7 (140 kDa), total STAT-1 (94/87 kDa) ISG-56 (56 kDa), total IRF-7 (51 kDa), and β-Tubulin (55 kDa) from whole brain lysates of WNV-infected WT and *Tlr8*$^{-/-}$ mice at day 4 p.i. (n = 6-8 per group). Primary mixed neuronal cultures isolated from WT and *Tlr8*$^{-/-}$ mice (6–12 month old, n = 3 per group) were cultured to maturity *in vitro* and infected with WNV (MOI = 1) for 24 hr. Gene expression of *Tlr7*

(F), *Irf-7* **(G)**, *Ifn-α* **(H)**, *Isg-56* **(I)**, and *WNV-E* **(J)** to *β-actin* were measured by qPCR. **(K)** WNV-infected neurons probed with anti-WNV-E (green) or anti-ISG-56 (red) antibodies were imaged using a confocal LSR 510 microscope at 100 × magnification. All qPCR assays were analyzed by a two-tailed Student's t-test (* denotes $p < 0.05$, and *ns* denotes non significant, ± 1 SEM). qPCR assays were performed three times and the immunoblotting assays were performed two times.

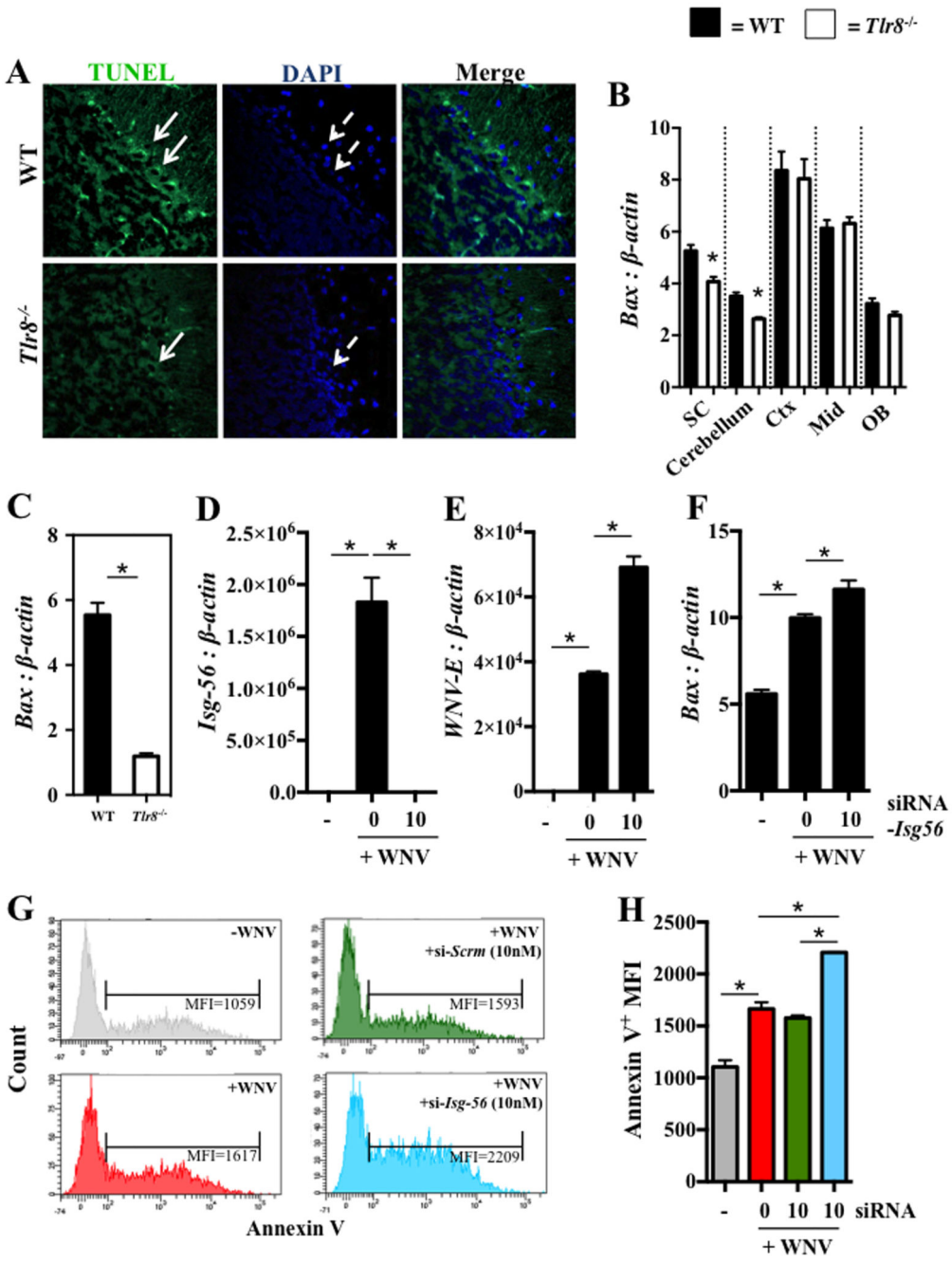

Figure 4. Reduced apoptosis in WNV-infected *Tlr8*$^{-/-}$ mice is localized to CNS-specific regions

(A) WT and *Tlr8*$^{-/-}$ mice brains were isolated at day 6 p.i. and imaged to detect cellular apoptosis in midsagittal brain sections. TUNEL labeling (green, white arrow) and DAPI (blue, dashed white arrow) were merged indicating reduced TUNEL immunofluorescence was observed in *Tlr8*$^{-/-}$ Purkinjie neurons of the cerebellum compared to WT controls (n = 4 per group). Gene expression profile of *Bax* **(B)** to *β-actin* in different brain regions: Cerebellum, Cortex (Ctx), Midbrain (Mid), Olfactory Bulb (OB), and spinal cords (SC) from WNV-infected WT and *Tlr8*$^{-/-}$ mice (n = 9-22 per group) at day 4 p.i. were analyzed by

qPCR. Primary mixed neuronal cultures isolated from WT and *Tlr8*$^{-/-}$ mice (6 to 12 month old, n = 3 per group) were cultured to maturity *in vitro* and infected with WNV (MOI = 1) for 24 hr. Gene expression of *Bax* **(C)** to *β-actin* was analyzed by qPCR. Gene expression of *Isg-56* **(D),** *WNV-E* **(E)** and *Bax* **(F)** were measured by qPCR in Neuro-2a cells transfected with siRNA targeting *Isg-56* (10 nM) for 24 hr, followed by infection with WNV (MOI = 5) for an additional 48 hr. **(G and H)** Neuro-2a cells were transfected with siRNA targeting *Isg-56* or with a scrambled siRNA control and infected with WNV, as above. Cells were stained with annexin V and PI followed by flow cytometric analysis (n = 3 per group). Brain sections were imaged using a confocal LSR 510 microscope at 63 × magnification. All qPCR and flow cytometric analyses were performed three times and analyzed using a two-tailed Student's *t*-test (* denotes $p < 0.05$, ± 1 SEM).

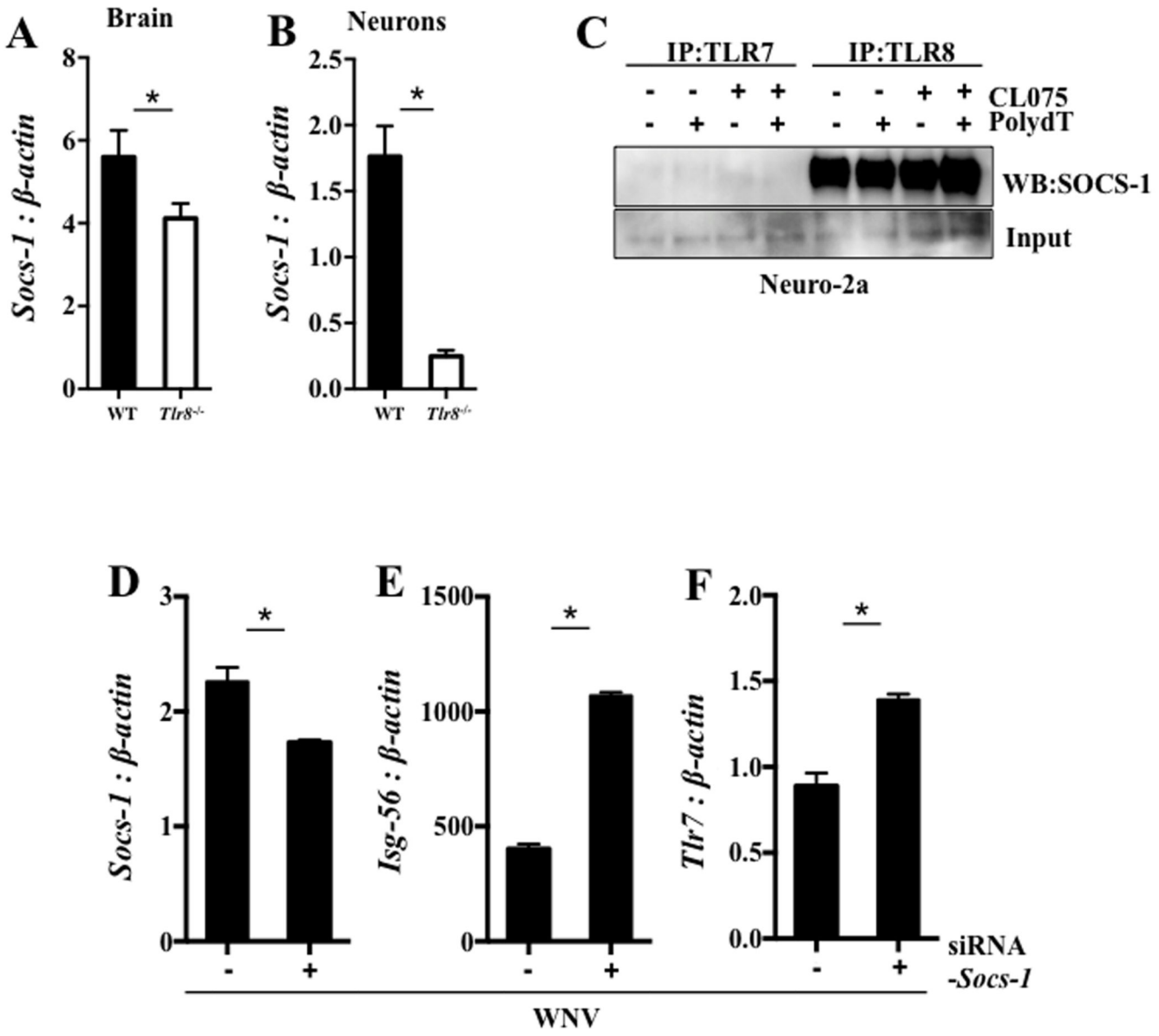

Figure 5. TLR8 signaling regulates Socs-1 expression

Gene expression of *Socs-1* **(A)** to *β-actin* (n = 6-8 per group) was analyzed in whole brains from WNV-infected WT and *Tlr8*$^{-/-}$ mice at day 4 p.i. by qPCR. Primary mixed neuronal cultures isolated from WT and *Tlr8*$^{-/-}$ mice (6 – 12 month old, n = 3 per group) were cultured to maturity *in vitro* and infected with WNV (MOI = 1) for 24 hr and gene expression of *Socs-1* **(B)** to *β-actin* was measured by qPCR. **(C)** Co-immunoprecipitation of TLR7 or TLR8 with SOCS-1 was performed in Neuro-2a cells stimulated with PolydT (10 μM), CL075 (10 μM) or both agonists for 24 hr by using anti-TLR7 or anti-TLR8 antibodies coated magnetic beads and Western blot analysis of SOCS-1. RAW 264.7 cells were transfected with siRNA targeting *Socs-1* followed by infection with WNV (MOI = 0.1) for 24hr and gene expression analysis of *Socs-1* **(D)**, *Isg-56* **(E)** and *Tlr7* **(F)** to *β-actin* was measured by qPCR. All qPCR assays were performed two independent times and analyzed

using a two-tailed, Student's *t*-test (* denotes $p < 0.05$, ± 1 SEM). Immunoprecipitation experiments were performed two times.

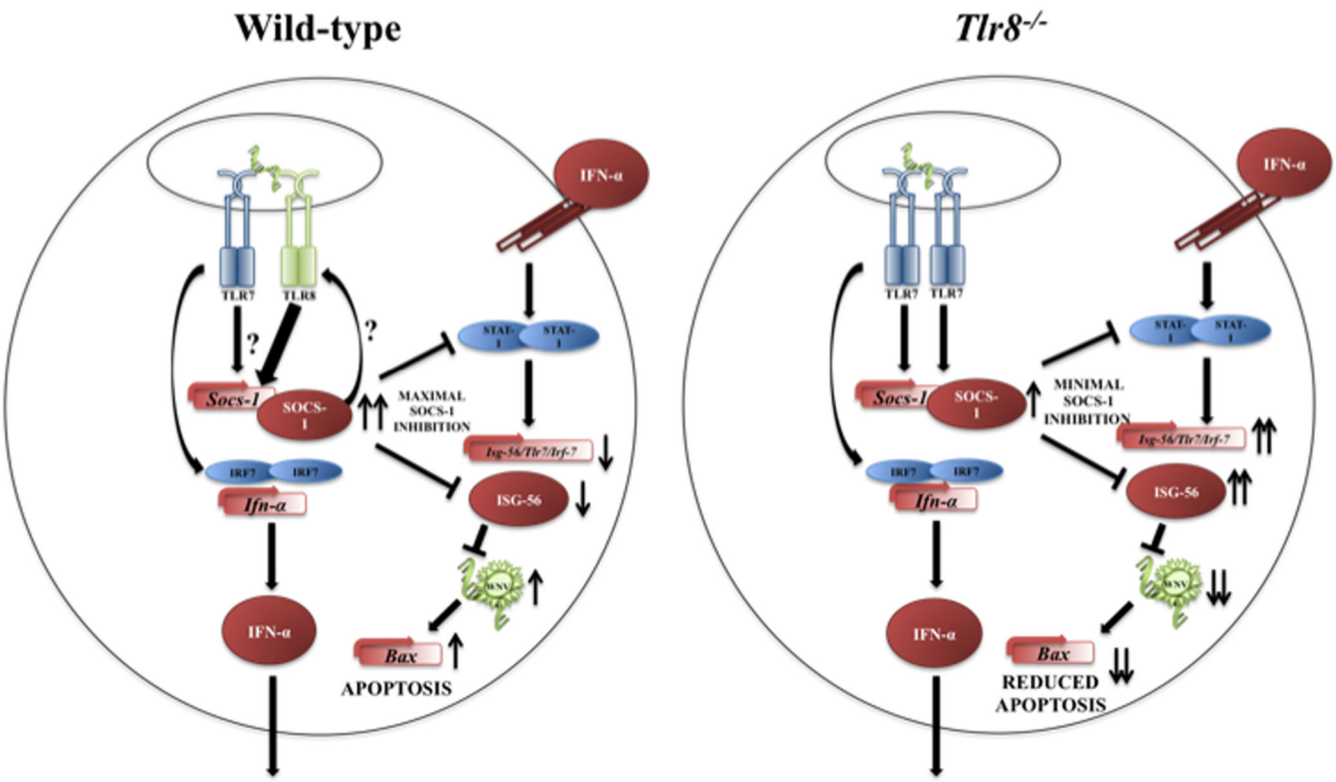

Figure 6. TLR8 signaling regulates SOCS-1 expression, leading to increased inhibition of antiviral immunity following WNV infection

Representative image of wild-type and *Tlr8*$^{-/-}$ mice cells that are infected with WNV and the proposed mechanism of signaling. In wild-type cells infected with WNV, TLR8 signaling results in increased SOCS-1, which negatively regulates antiviral immunity via direct STAT-1 inhibition (58) or possibly through ISG-56 inhibition, which results in increased viral load, triggering the p53-Bax-dependant apoptosis pathway (50, 51). Conversely, in TLR8 deficient cells (*Tlr8*$^{-/-}$) SOCS-1 is not adequately induced, therefore antiviral immunity is minimally inhibited, resulting in increased *Isg-56*, *Irf7*, and *Tlr7* expression, which ultimately amplifies the TLR7 signaling pathway, while successfully controlling viral load and reducing virus-induced apoptosis. The non-canonical function of SOCS-1 directly binding to TLR8 and not TLR7, in both mock and TLR7 and TLR8 stimulated cells, is yet to be further elucidated.